Pathways of Viologen-Mediated Oxidation-Reduction Reactions across Dihexadecyl Phosphate Bilayer Membranes

Brian C. Patterson and James K. Hurst*

Department of Chemical & Biological Sciences, Oregon Graduate Institute of Science & Technology, Beaverton, Oregon 97006-1999

Received: July 17, 1992; In Final Form: October 19, 1992

Transmembrane reduction of methylviologen (*N*,*N*-dimethyl-4,4′-bipyridinium, MV^{2+}) and several *n*-alkylmethyl analogs, i.e., *N*-alkyl-*N*′-methyl-4,4′-bipyridinium (C_nMV^{2+}, $n \leq 10$), entrapped within dihexadecyl phosphate (DHP) vesicles by $S_2O_4^{2-}$ or $CrEDTA^{2-}$ located in the bulk aqueous phase occurred only when viologens were also initially present on the same side of the membrane as the reductant. Viologen radical cation formation was biphasic, with reduction of the externally bound viologen dications preceding reduction of the entrapped viologen. For MV^{2+}, the rate law was $d[MV^+]/dt = k_a[MV^{2+}]_o[SO^{2-}]_o + k_b[MV^+]_o[MV^{2+}]_i$, where the subscripts i and o refer to viologens bound at the vesicle inner and outer interfaces, respectively. Transmembrane reduction was accompanied by comigration of a viologen radical cation with each electron transferred across the bilayer. The MV^+ ion formed on the external surface was monomeric, but the MV^+ formed internally was aggregated (or multimeric); from the wavelength dependence of the kinetic curves, it was shown that aggregation coincided with or rapidly followed the rate-limiting transmembrane redox step. For the C_nMV^{2+} ions, the reaction dynamics were qualitatively similar but were complicated by the simultaneous presence of both monomeric and multimeric forms of C_nMV^+ at the outer vesicle interface. When $n > 10$, reduction of external C_nMV^{2+} ions was biphasic. For $C_{16}MV^{2+}$, only about one-third of the entrapped viologen was reducible unless the reaction medium also contained lipophilic ions, under which conditions all of the internal ions could be reduced. Correspondingly, only one-third of the external $C_{16}MV^{2+}$ translocated to the inner vesicle surface. Computer simulations of the complex kinetic waveforms required inclusion of two independent transmembrane redox steps to obtain adequate data fits. There were interpreted in terms of two distinct reaction pathways involving (i) transverse diffusion of interfacially bound reactants and (ii) electron tunneling between the viologen radical cations and dications juxtaposed in the opposite bilayer leaflets. Possible alternative molecular mechanisms corresponding to the two pathways are discussed.

Introduction

Oxidation-reduction reactions between redox ions bound at the opposite interfaces of vesicle bilayer membranes have been documented for numerous systems.[1] These reactions are remarkable because they imply charge transfer through an insulating barrier of ~40-Å thickness, the approximate width of the membrane hydrocarbon phase. The molecular mechanisms of these types of reactions are generally not well understood.[1a] Two limiting pathways that have been advanced are (i) that the membrane-bound redox mediator functions as a membrane-permeable electron shuttle, alternately undergoing oxidation and reduction at the opposite aqueous-hydrocarbon interfaces, and (ii) that reaction occurs by electron transfer through the bilayer between reactants localized in the opposite bilayer leaflets. The extent to which molecular diffusion and long-range electron transfer contribute to the overall pathway has not been firmly established in any real system[2] although, given sufficient information about the spatial localization and diffusional properties of the amphiphilic redox components, it is possible in principle to distinguish between the two limiting pathways.[1a]

To address these mechanistic issues, we have undertaken systematic study of the structural and dynamical properties of conceptually simple systems comprising DHP vesicle-bound monoalkylviologens (C_nMV^{2+}; *N*-*n*-alkyl-*N*′-methyl-4,4′-bipyridinium ions). At least two binding configurations can be distinguished from the physical properties of these particles, the critical determinant being the length of the *n*-alkyl substituent. Specifically, (i) externally bound C_nMV^{2+} ions with carbon chain lengths (*n*) shorter than 10 methylene units were easily removed by cation-exchange chromatography, but the long-chain analogs ($n > 10$) could not be removed by this method; (ii) incremental addition of C_nMV^{2+} with $n > 10$ to preformed DHP vesicles caused progressive swelling, whereas swelling did not occur when $n \leq 10$;[3] (iii) $C_nMV^{2+/+}$ one-electron reduction potentials showed a discontinuous shift of −100 mV upon increasing the chain length from $n = 10$ to $n = 12$ that was not observed for potentials measured in other vesicles or in homogeneous solution;[4] (iv) bathochromic shifts in ultraviolet adsorption bands observed upon binding to DHP were greater for the long-chain analogs than the short-chain analogs, consistent with transfer of the long-chain viologens to a less polar environment; (v) short-chain C_nMV^+ radical ions generated by photoreduction of frozen C_nMV^{2+}–DHP suspensions were more exposed to solvent than long-chain C_nMV^+ ions, as determined by electron spin-echo modulation spectroscopy in D_2O, whereas no differences were detected in other types of microphases.[5] Strong binding of the short-chain C_nMV^{2+} ions to DHP has been confirmed by equilibrium dialysis[4] and gel permeation chromatography.[6] Collectively, these data have been interpreted to indicate that when $n > 10$, the C_nMV^{2+} alkyl chains interpenetrate the membrane hydrocarbon phase forming part of the bilayer structure. In contrast, the shorter-chain viologens are thought to be only electrostatically bound to anionic phosphate headgroups at the aqueous-hydrocarbon interface. This binding model is consistent with kinetic experiments which indicated that the DHP-bound short-chain viologens were more reactive toward aqueous-phase reductants.[7-9] A complication evident in the studies with long-chain viologens ($n > 10$) was the existence of two distinct subpopulations with differing reactivities.[7,8] Photochemical reactions of other DHP-bound donor and acceptor molecules also exhibit complex kinetics that have been attributed to microscopic binding heterogeneities.[6,10] We report herein

* Corresponding author.

0022-3654/58/2097-0454$04.00/0

studies on C_nMV^+-mediated transmembrane reduction of C_nMV^{2+} ions by membrane-impermeable reductants. Measurement of reaction rates and topographic redistributions of C_nMV^{2+} ions have provided the basis for assigning reaction pathways. These assignments are consistent with recently measured membrane permeabilities of the C_nMV^{2+} and C_nMV^+ ions.[11]

Experimental Section

Materials. The chloride salts of *N*-alkyl-*N'*-methyl-4,4'-bipyridinium (C_nMV^{2+}) and *N*-methyl-4,4'-bipyridinium (MB^+) ions were synthesized by Dr. David H. Thompson at OGI following previously established procedures.[3] Purities of these compounds were established by ^1H NMR spectroscopy and thin-layer chromatography on silica gel using 3:3:1 methanol:H_2O:50% ethylammonium chloride as the mobile phase. Anaerobic solutions of the reductant $Cr^{II}(EDTA)^{2-}$ were prepared by reducing 10 mM $Cr(ClO_4)_3$ in 20 mM KCl, pH 3.0 (HCl), over zinc amalgam until the color changed to pale blue, indicating complete reduction to chromous ion, followed by adding 2-fold volume excess of an anaerobic solution of 10 mM disodium EDTA to give a 3.3 mM $Cr^{II}(EDTA)^{2-}$ solution. Stock solutions of $Na_2S_2O_4$ were prepared by dissolving the solid in deoxygenated solutions of 4–8 mM Tris-HCl or imidazole-HCl, pH 8.0; $S_2O_4^{2-}$ concentrations were determined spectrophotometrically at 315 nm ($\epsilon = 6.9 \times 10^3$ M^{-1} cm^{-1}).[12] Other chemicals were best-available grades from commercial suppliers and used as received. Critical experiments were checked using dihexadecyl phosphate that had been twice recrystallized from methanol; results obtained were identical to those obtained with commercial DHP. Water was purified using a reverse osmosis/deionization system.

Vesicle Preparation. DHP small unilamellar vesicles (SUV) were prepared by ultrasonication of buffer suspensions of the solid essentially as previously described.[3] Vesicles incorporating viologens were prepared by including the viologen in the buffer; vesicles containing viologens bound only at the external interface were prepared by flow-mixing viologen solutions with solutions containing preformed vesicles.[3] Vesicles containing other asymmetric distributions of reactants were prepared by column chromatography using either gel exclusion or ion exchange, depending upon the strength of ion binding to the vesicles. Methylviologen dication was removed from the external medium by exclusion chromatography on Sephadex G-50 Fine gels that had been hydrated in the medium buffer and poured into a 2.6 × 45 cm column. Cation-exchange chromatography on a Chelex 100 column (1.5 × 20 cm) was used to remove short-chain C_nMV^{2+} from the external surface of DHP vesicles. This exchanger was capable of removing nearly all externally bound viologens with alkyl chain lengths up to 10 carbons in a single pass, whereas the longer-chain analogs were retained nearly quantitatively by the vesicles following passage down the columns. The Chelex 100 resin was acid–base cycled with 1 N HCl and 1 N NaOH, then flushed with 0.5 M buffer at its pK_a, and equilibrated with the actual medium buffer prior to chromatography. The void volumes of both gel and ion-exchange columns were determined with Blue Dextran (MW 2×10^6). Vesicle-containing solutions were then loaded onto the columns; following elution of the void volume, the eluant fraction containing the vesicles was collected. Phosphate analyses, described below, indicated that the vesicle number densities decreased by approximately 2-fold and 20%, respectively, on passage through the gel and ion-exchange columns. Removal of external ions was confirmed spectrophotometrically by adding the reductant, $S_2O_4^{2-}$, to the vesicle eluent fractions under anaerobic conditions. No immediate loss was observed in the residual absorbances at 260 nm, the approximate band maximum for the C_nMV^{2+} ions, indicating that they were not accessible to the externally added reductant. Furthermore, absorption increases observed in the vicinity of 604 nm, the spectral maxima of the C_nMV^+ radical cations, amounted to only a few percent of the total C_nMV^{2+} present. For these measurements, SUV suspensions at the same number densities as the samples but containing no viologen were used as reference solutions. Although light scattering from these SUV is small above 206 nm,[3] this procedure corrected for turbidities arising from this source. The band maxima for DHP-bound C_nMV^{2+} ions shifted progressively 3–7 nm to longer wavelengths as the chain lengthened. The molar absorption coefficients at the maxima were nearly constant, however;[7] an average value of 2.2×10^4 M^{-1} cm^{-1} was taken for these calculations. In aqueous solution, the band maximum for all of the viologen dications appeared at 258 nm.

Analytical Methods. Lipid concentrations were routinely determined by measuring the inorganic phosphate concentration following mineralization under strong oxidizing conditions.[13] The phosphorus assay involved formation of phosphomolybdate and its subsequent complexation with Malachite Green. The absorbance developing in 10 min at 623 nm was recorded and compared to a calibration curve constructed using known amounts of Na_2HPO_4 to determine the phosphorus concentration. The extent of C_nMV^{2+} ion binding to DHP SUV was determined by equilibrium dialysis using cells consisting of two 5-mL chambers separated by a Scienceware No. 40299 cellulose membrane (6000-nm cutoff). Typically, one chamber was nearly filled with the DHP vesicles and the other chamber with an equal volume of the viologen in an identical buffer solution. The dialysis cell was then mounted on a slowly moving shaker, and the compartmentalized solutions were allowed to equilibrate overnight. Control experiments made in the absence of DHP vesicles established that equilibration was complete within 8 h. It was also found that 5–10% of the added viologen adhered to the dialysis membrane. Following equilibration, the concentration of viologen in each chamber was determined spectrophotometrically, from which the amount of free and vesicle-bound viologen was calculated.

Instrumentation and Data Analysis. Fluorescence spectra were determined using a Perkin-Elmer MPF-66 spectrofluorimeter interfaced to a PE7500 computer. Optical absorption spectra were determined using either Perkin-Elmer Lambda 9 or Hewlett-Packard 8452A spectrophotometers; the latter instrument was interfaced to a ChemStation data acquisition/analysis system. A home-built Gibson-type stopped-flow apparatus was used to measure reaction dynamics. This apparatus, which was specifically designed for handling anaerobic solutions,[7,14,15] was fitted with three reagent reservoirs that could be purged of oxygen by sparging with inert gases. Immediately prior to initiating a run, a concentrated solution of the oxygen-sensitive reductant was diluted into deoxygenated buffer in one reservoir and its concentration determined spectrophotometrically. Air was then swept from the apparatus using deoxygenated buffer from a second reservoir; the reactant solutions were loaded into the drive syringes and mixed by passage through a tangential 12-jet flow cell. Reaction dynamics were followed by observing transmittance decreases at selected wavelengths in the visible to near-ultraviolet region corresponding to formation of C_nMV^+ radical cations. Voltage–time waveforms were recorded on a Nicolet 4094B digital oscilloscope equipped with a 4568 plug-in interfaced to a DEC PRO-350 computer. Data were analyzed using either an adaptation[14] of the program CURFIT by Bevington[16] based upon an algorithm by Marquardt, which treats the waveform after conversion to absorbance as series of exponential functions, or a general simulation program[14] for which measured absorbances were compared to calculated data for any given mechanism consisting of a series of steps with any specified reaction order. The programs were run using the RT-11 operating system; 794-3968 individual data points were used in analyses of individual kinetic traces. Goodness of fit was evaluated quantitatively by a χ^2 statistic and qualitatively by plotting the random residual

for best-fit lines and the actual data. All kinetic measurements were made at 23 °C.

Results

Viologen Binding to DHP Vesicles. We have found that vesicle binding by C_nMV^{2+} and similar polyvalent amphiphiles[4,17] often cannot be quantitatively described by simple Langmuir or Stern adsorption isotherms.[18] Failure of these models might be ascribed to the assumption that the amphiphilic electrostatic charge is distributed uniformly over the membrane surface and that cooperative or other anticooperative forces are absent, which would be particularly inappropriate in instances where evidence of dopant aggregation or lateral phase separation existed. As described below, aggregation of a portion of the DHP-bound C_nMV^+ radical cations formed by one-electron reduction of the corresponding dications was apparent from their absorption spectra. Lacking a quantitative model, we have determined directly the extent of C_nMV^{2+} ion binding to DHP vesicles under the conditions of the kinetic experiments. For the ions with n = 10–16, binding exceeded 97% under all relevant experimental conditions, which included binding ratios as high as C_nMV^{2+}/DHP = 0.12. For the shorter chain analogs, the extent of binding was dependent upon the viologen loading. For C_6MV^{2+}, binding varied from 76% to 55% over the range C_6MV^{2+}/DHP = 0.04–0.12 in 20 mM Tris, pH 8.0; corresponding values for C_8MV^{2+} were 92–84% and 0.04–0.17. The C_nMV^{2+}/DHP ratios are expressed as mole fractions and can be converted to average number of viologen ions bound per vesicle by multiplication by 3.9×10^3, the vesicle aggregation number.[3] Brief investigation of methylviologen binding to DHP vesicles over a wider range of conditions showed that the extent of association was dependent upon the solution pH and ionic strength, as well as the MV^{2+} to DHP ratio. In 20 mM Tris, pH 8.0, binding varied from 80% to 43% as the MV^{2+}/DHP ratio increased from 0.026 to 0.10; in 20 mM glycine, pH 9.5, with MV^{2+}/DHP $\simeq$ 0.05, binding was 86%, and in H_2O using DHP vesicles whose phosphate group headgroups were neutralized with sodium hydroxide, MV^{2+} binding has been reported as essentially complete.[19] These effects can be understood qualitatively in terms of changes in electrostatic binding forces. Specifically, decreasing the solution ionic strength and increasing in alkalinity should increase the effective negative surface charge density of the anionic DHP vesicles, enhancing electrostatic attraction of the dications. In general, viologen radical cations are considerably more lipophilic than their corresponding dications, as demonstrated by their increased partitioning into the organic phase in bulk two-phase distribution experiments[20,21] and greater solubilities in monoionic micelles.[22,23] Based upon the vesicle binding properties of the dications, all of the radical cations formed in the reactions under investigation can be considered as completely DHP associated.

The distributions of short-chain C_nMV^{2+} ions between inner and outer vesicle surfaces obtained when the vesicles were formed in viologen-containing solutions were determined by cation-exchange chromatography. Viologen content was measured spectrophotometrically before and after passage through a Chelex 100 column. Differences were corrected for vesicle dilution, as determined by phosphate analysis, and residual viologen remaining on the outer surface (typically less than 4% for $n \leq 10$) was determined by adding $S_2O_4^{2-}$ to anaerobic solutions. Inside: outside distributions calculated from the data were as follows: for MV^{2+}, 30:70%; for C_6MV^{2+}, 32:68%; for C_8MV^{2+}, 34:66%; and for $C_{10}MV^{2+}$, 32:68%. The medium was 20 mM Tris-HCl, pH 8.0, with C_nMV^{2+}/DHP ratios set at 0.04–0.06. These values are nearly identical to the relative inner and outer surface areas of the vesicles. Prepared and isolated as described in the Experimental Section, DHP SUV are a unimodal distribution of spherical particles with mean hydrodynamic radii of about 13 nm.[3] Assuming a bilayer width of 4 nm, the percentage of total inner and outer surface areas is calculated to be 32:68%. Thus, the C_nMV^{2+} ions appear to distribute in a statistically random fashion over all membrane surfaces when the vesicles are formed in the presence of the viologen dications. The slightly lower percentage of encapsulation of MV^{2+} probably reflects its incomplete binding to the vesicles. With DHP surfactant concentrations of 2–8 mM, the amount of solution occluded by the vesicles is only 0.1–0.4% of the total solution volume. If the viologens were not DHP bound, the amount of entrapped material would be dictated by the relative volumes of internal and external solution and, hence, would have been minuscule.

Dithionite Reduction of Vesicles Containing Externally Bound C_nMV^{2+} Ions. *a. Reaction Stoichiometries.* One-electron reduction of DHP-bound viologen by $S_2O_4^{2-}$ ion can be described by the reaction

$$C_nMV^{2+}\text{–DHP} + (1/2)S_2O_4^{2-} + H_2O \rightarrow C_nMV^{+}\text{–DHP} + SO_3^{2-} + 2H^+ \quad (1)$$

Based upon optical spectroscopic changes, viologen reduction was complete when dithionite was in 10–30-fold excess at pH 7.5–8.0, but only partial reduction occurred in more acidic media. This behavior can be understood from consideration of the reactant reduction potentials. From data reported by Mayhew,[24] the midpoint potential for the $SO_3^{2-}/S_2O_4^{2-}$ half-reaction was calculated to be –463 mV (vs NHE) at pH 7.5 and –522 mV at pH 8.0; one-electron reduction potentials for C_nMV^{2+}–DHP under comparable conditions range from –401 mV for $C_{10}MV^{2+/+}$ to –508 mV for $C_{16}MV^{2+/+}$.[4] Calculated radical cation/dication equilibrium ratios varied from $[C_{16}MV^+\text{–DHP}]/[C_{16}MV^{2+}\text{–DHP}] \geq 55$ at pH 7.5 to $[C_{10}MV^+]/[C_{10}MV^{2+}] \geq 3.6 \times 10^4$ at pH 8.0, the conditions of the kinetic experiments reported herein. In contrast, with HSO^{3-} as the oxidized product and assuming the $C_nMV^{2+/+}$ potentials are pH-independent, the corresponding calculated ratios ranged from 0.06 to 1.0 at pH 5.0, predicting only 6–50% conversion to the radical cations in the more acidic environment. Also, because the one-electron reduction potentials for the DHP-bound radical cations are 260–350 mV more negative than for the dications,[4] further reduction to the C_nMV^0 diradical species was inappreciable under all reaction conditions investigated; i.e., calculated limiting ratios were $[C_{16}MV^0]/[C_{16}MV^+] \leq 2.8 \times 10^{-3}$ at pH 7.5 and $[C_8MV^0]/[C_8MV^+] \leq 0.1$ at pH 8.0. Thus, eq 1 accurately describes the overall reactions anticipated from the thermodynamic potentials. It might be noted that, because the $SO_3^{2-}/S_2O_4^{2-}$ potential is sensitive to the SO_3^{2-} concentration under the conditions of our experiments, use of relatively pure $Na_2S_2O_4$ reagent was necessary to ensure complete reduction of $C_{16}MV^{2+}$–DHP and other long-chain analogs to their radical cations.

The MV^+ radical cation formed was visually the pure blue color associated with the monomeric form.[25] Careful examination of its optical spectrum at various DHP loadings indicated a small contribution from the purple multimeric form whose concentration increased with increasing MV^+/DHP ratios (Figure 1). The extent of aggregation increased progressively at equivalent loadings with increasing viologen alkyl chain length until, with $C_{16}MV^+$–DHP, the contribution of the multimer was clearly evident in the optical spectra of product solutions. Identical isosbestic points were observed at 371, 552, and 760 nm in the spectra for the DHP-bound MV^+ and $C_{16}MV^+$ radical cations, suggesting that the spectra of the individual components were very nearly identical. A monomer "reference" spectrum was obtained by reducing 11 μM aqueous MV^{2+} in a 10-cm-path length optical cell; this spectrum was devoid of absorbance at 1000 nm where the multimer had significant absorbance ($\epsilon_{1000} \simeq 4.2 \times 10^3$ M^{-1} cm^{-1}, Figure 1) and was, therefore, judged to be at least 90% monomeric. A multimer "reference" spectrum was obtained by partial reduction of aqueous $C_{16}MV^{2+}$ with $S_2O_4^{2-}$ ion; this spectrum was characterized by almost complete disap-

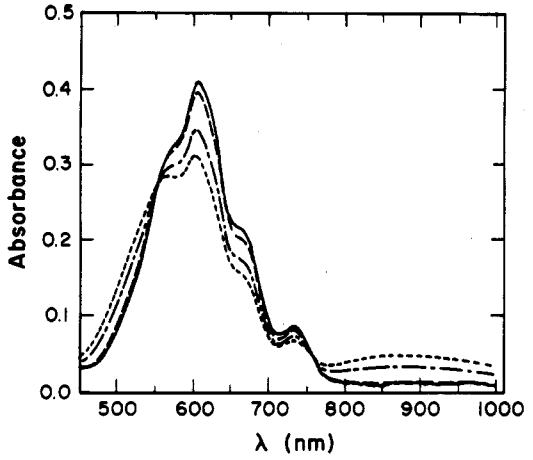

Figure 1. Visible–near-infrared optical spectra of dithionite-reduced MV^{2+} ion adsorbed onto DHP vesicles. Conditions: 4 mM DHP in 20 mM Tris-HCl, pH 8.0; MV^{2+}/DHP = 0.0022 (solid line), 0.0075 (dashed line), 0.028 (dot-dashed line), and 0.056 (dotted line). All spectra were scaled to an equivalent MV^{2+} concentration of 30 μM (MV^{2+}/DHP = 0.0075). Isosbestic points are at 552 and 760 nm.

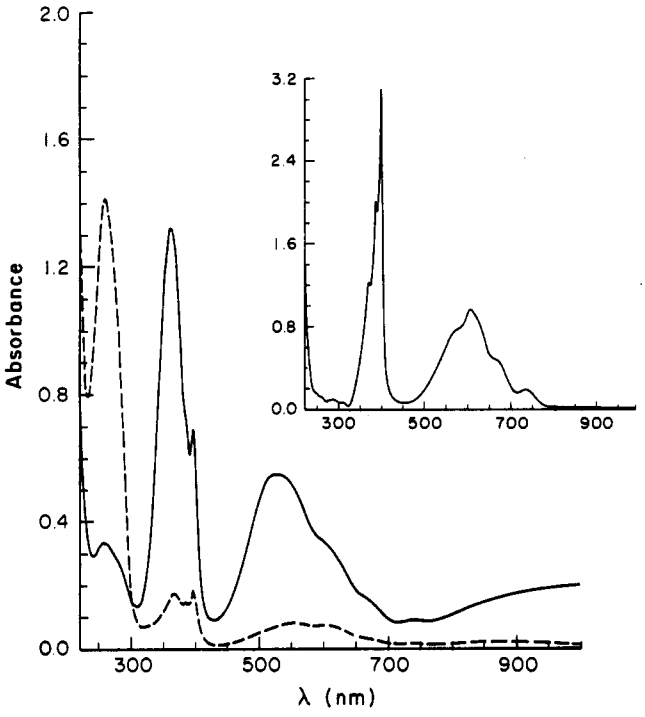

Figure 2. Product spectra from dithionite reduction of DHP vesicles initially containing 30 μM MV^{2+} bound at both inner and outer surfaces: solid line, initial reduction following addition of 5-fold excess of $S_2O_4^{2-}$ ion; dashed line, second reduction following oxygenation and purging with argon; inset, subsequent anaerobic addition of sodium dodecyl sulfate to the redox cycled solution containing $S_2O_4^{2-}$ ion. The absorption band at 260 nm is due to the MV^{2+} ion.

pearance of the sharp monomer peak at 397 nm (Figure 2, inset). Using these two spectra, an empirical formula was derived for the fraction of monomer present in any given viologen radical spectrum, i.e., fraction monomer = $(Abs_{605}/Abs_{552} - 0.59)/0.98$. Since isosbestic points and peak maxima were indistinguishable for the radical cations in aqueous solution and externally bound to DHP, this formula is valid for both environments.

b. Reduction Kinetics. Dithionite reduction of C_nMV^{2+} ions adsorbed to the external surface of DHP SUV has been extensively studied in 20 mM Tris-HCl, pH 8.0.[7] The reaction exhibited one-half-order dependence upon $[S_2O_4^{2-}]$, indicating that the SO^{2-} ion formed by dithionite dissociation is the actual reductant.[26,27] For the short-chain analogs ($n \leq 10$), the reaction was first-order in C_nMV^{2+}; when $n \geq 12$, two concurrent pseudo-first-order pathways were evident, indicating that the long-chain C_nMV^{2+} ions were bound in two kinetically distinct reaction environments.[7] These observations were confirmed in the present study. For reasons indicated in a subsequent section, it was also necessary to determine kinetic parameters for reactions of the long-chain viologens in 75 mM imidazole buffer, pH 7.5. These reactions were measured using stopped-flow spectrophotometry by monitoring the appearance of C_nMV^+ ion at the monomer–multimer isosbestic point, for which $\epsilon_{552} = 9.3 \times 10^3$ M^{-1} cm^{-1}. With reductant in excess, the rate law was the same as previously determined, i.e.

$$d[C_nMV^+]/dt = (k_1[C_nMV^{2+}] + k_2[C_nMV^{2+}])[S_2O_4^{2-}]^{1/2} \quad (2)$$

Rate constants and relative amplitudes (A_1/A_2) obtained for the two steps at 23 °C were as follows: for $C_{12}MV^{2+}$, $k_1' = 7.0$ (±0.6) × 10^6 M^{-1} s^{-1}; $k_2' = 2.7$ (±0.4) × 10^6 M^{-1} s^{-1}, $A_1/A_2 = 0.37/0.63$; for $C_{16}MV^{2+}$, $k_1' = 1.3$ (±0.3) × 10^6 M^{-1} s^{-1}; $k_2' = 0.2$ (±0.02) × 10^6 M^{-1} s^{-1}, $A_1/A_2 = 0.10/0.90$. The constants reported are for the bimolecular reaction between C_nMV^{2+}–DHP and SO^{2-}, given by $k' = k/K$, where $K = 1.4 \times 10^{-9}$ M is the constant for homolytic dissociation of $S_2O_4^{2-}$ to SO^{2-}.[24] The values are 2–3-fold greater than reported for 20 mM Tris, pH 8.0, which is about 3-fold less than expected on the basis of ionic strength differences alone, as reported for $C_{16}MV^{2+}$–DHP.[8] Relative amplitudes for the fast and slow components were also similar to values reported for Tris-HCl buffered media. No systematic variation in rate constants with the extent of viologen loading was observed over an experimental range encompassing C_nMV^{2+}/DHP = 0.015–0.033.

Transmembrane Reduction of MV^{2+} Ion. *a. Reaction Stoichiometries.* When MV^{2+} or the short-chain C_nMV^{2+} analogs were entrapped within DHP vesicles with viologen removed from the outer surface, virtually no radical cations were formed upon adding $S_2O_4^{2-}$ ion to the bulk solution. When C_nMV^{2+} ions were also present at the outer interface before reduction, $S_2O_4^{2-}$ addition caused reduction of both the external viologen and some or all of the internal viologen. This behavior indicates that external viologen molecules were able to mediate transmembrane viologen reduction by dithionite ion.

The stoichiometry of the transmembrane redox step depended upon the C_nMV^{2+} identity, its inner-to-outer interfacial distribution, and, in some instances, the total viologen concentration. For MV^{2+}, when the total concentration of encapsulated viologen equaled or exceeded the external viologen concentration, one-to-one correspondence was observed between the number of inner viologen ions reduced and the number of MV^{2+} ions initially present on the outer surface. Typical data for a series of runs in which incremental additions of MV^{2+} were made to a suspension of DHP particles containing entrapped MV^{2+} are given in Table I. When the amount of external MV^{2+} exceeded the inner MV^{2+}, all of the MV^{2+} in the system was dithionite-reducible.

Reduction of internally localized viologens was accompanied by inward translocation of C_nMV^+ ions from the outer vesicle surface. This phenomenon was first noted in experiments involving repetitive reduction–oxidation cycling of MV^{2+}-containing DHP vesicles with $S_2O_4^{2-}$ and O_2.[28] As illustrated in Figure 2, $S_2O_4^{2-}$ reduction of DHP vesicles containing equimolar internal and external MV^{2+} gave essentially complete reduction to MV^+, as determined spectrophotometrically. Aerobic oxidation gave quantitative recovery of the dication, as determined by measurement of the absorbance at 260 nm. However, following repurging with argon, addition of a second aliquot of $S_2O_4^{2-}$ gave less than 10% reduction to the radical cation (Figure 2, dashed line); subsequent addition of an anaerobic solution of sodium dodecyl sulfate to disrupt the vesicles caused immediate, quantitative reduction to the radical cation (Figure 2, inset). It appeared, therefore, that during the first reductive step the external

TABLE I: Reaction Stoichiometry, Product Composition, and Topographic Redistribution following MV^+-Mediated Transmembrane Reduction of MV^{2+} Ion[a]

$[MV^{2+}]_i$[b] (μM)	$[MV^{2+}]_o$[b] (μM)	$[MV^+]$[c] (μM)	$\Delta[MV^{2+}]_i$[d] (μM)	$[MV^+]/[MV^{2+}]_o$
		A. $[MV^{2+}]_i > [MV^{2+}]_o$		
21	16	32	14	2.0
28	25	46	21	1.8
31	22	43	24	2.0
31	16	31	12	1.9
46	10	22	nd[h]	2.2
46	14	30	nd	2.1
46	19	40	nd	2.1
46	25	52	nd	2.1
46	34	66	nd	1.9
		B. $[MV^{2+}]_i < [MV^{2+}]_o$		
31	59	90	24[f]	48[e]
31	59	90	41	48[e]
31	59	90	42[g]	48[e]

[a] Conditions: 3–4 mM DHP in 20 mM Tris-HCl, pH 8.0, 5-fold excess $S_2O_4^{2-}$ ion added, except where noted. [b] Initial concentrations of internally (i) and externally (o) bound MV^{2+} ions. [c] Total MV^{2+} formed upon $S_2O_4^{2-}$ addition, determined spectrophotometrically. [d] MV^{2+} accumulated, determined by reduction–oxygenation cycling followed by chromatographic removal of external MV^{2+} ions. [e] Percent multimer; estimated spectrophotometrically according to empirical equations given in the text. [f] A 1-fold excess of $S_2O_4^{2-}$. [g] A 10-fold excess of $S_2O_4^{2-}$. [h] Not determined.

MV^+ cations had diffused across the bilayer and were subsequently trapped inside the vesicle upon oxygenation. This inference was confirmed by both cation-exchange chromatography and equilibrium dialysis, which demonstrated that after one reduction–oxygenation cycle the MV^{2+} could no longer be removed from the vesicles.

A remarkable feature of these reactions is that the DHP-encapsulated MV^+ ion gave an absorption spectrum indicating near-quantitative formation of the multimeric form of the radical. In other environments, e.g., homogeneous solution or bound at the DHP outer interface (cf. Figures 1 and 2), the monomeric form predominated at these concentration levels. The multimer spectrum of this species was different from that formed on DHP vesicle external surfaces at higher loadings. The isosbestic point was determined to be 546 nm (rather than 552 nm) by varying inner and outer viologen concentration ratios under conditions that caused extensive changes in the relative amounts of monomer and multimer formed; the isosbestic extinction coefficient was $\epsilon_{546} = 8.2 \times 10^3\ M^{-1}\ cm^{-1}$. An apparent pure dimer spectrum was obtained by digitally subtracting from the observed spectra a monomer spectrum sufficient to remove the characteristic monomer peak at 397 nm. This calculated spectrum was very similar to the other multimer spectrum but had peak maxima at 358 and 519 nm. Using the calculated multimer and normal MV^+ monomer spectra, an empirical formula was derived for the fraction of MV^+ present as monomer in a given viologen radical spectrum where transmembrane redox had occurred, i.e., fraction monomer = $(Abs_{605}/Abs_{546} - 0.41)/1.20$. This equation is valid only for systems containing monomer and internally localized multimer. For vesicles containing the long-chain C_nMV^+ analogs at both interfaces, two spectroscopically distinct forms of the dimer coexisted with the monomer; in such systems, an isosbestic point was no longer present.

When the initial internal MV^{2+} equaled or exceeded the external concentration, all of the external MV^+ formed was taken up by the vesicles. Therefore, stoichiometric measurements of MV^+ ions translocated per electron were made under conditions where the initial external MV^{2+} exceeded the internal MV^{2+} concentration. The final distribution following reduction–oxidation cycling determined by chromatography was dependent upon the molar excess of $S_2O_4^{2-}$ present in solution (Table I). As will be discussed, this effect is probably a consequence of redox "pumping" arising from repetitive cyclic oxidation–reduction occurring during the relatively lengthy time required to aerobically oxidize the $S_2O_4^{2-}$ ion. A better estimate of the reaction stoichiometry could be made from the spectrally determined percentage of dimer formed in the reductive half-cycle. This value was independent of the amount of $S_2O_4^{2-}$ ion added in excess (Table I); based upon spectra obtained with internal MV^{2+} in excess (e.g., Figure 2), approximately 80% of the internal MV^+ was multimeric at these DHP vesicle loadings. Assuming that the external MV^+ was completely monomeric, spectral calculations indicated that about 60% (or 54 μM) of the total MV^+ was located inside the vesicle following reduction. This value corresponds to uptake of 0.74 MV^+ per electron translocated. Experimental data obtained for other reaction conditions gave similar or higher ratios, indicating that, by the criterion of optical spectroscopy, very nearly one MV^+ was taken up by the vesicles for every internal MV^{2+} ion reduced.

The (ethylenediaminetetraacetato)chromium(II) ion was used as an alternate reductant. As with $S_2O_4^{2-}$, transmembrane reduction of internal MV^{2+} was not observed unless MV^{2+} was also initially present at the outer vesicle interface. Reduction stoichiometries and the extent of MV^{2+} dimerization and net translocation were identical within experimental uncertainty to values obtained with dithionite ion.

No net translocation of DHP-bound MV^{2+} dication was detected in redox cycling experiments when the membrane-impermeable oxidant,[6,18] ferricyanide ion, was used in place of O_2. Oxidation of $S_2O_4^{2-}$-reduced vesicle suspensions containing predominantly multimeric, hence internally localized, MV^+ gave product solutions in which one-half of the MV^{2+} product ion was external. The overall rate of reoxidation was slow, requiring 5–10 s for completion as opposed to 10^2-fold faster rates for oxidation of DHP vesicles containing externally bound C_nMV^{2+} ions or for $Fe(CN)_6^{3-}$ oxidation of MV^+ in homogeneous solution.[29] These results imply that the inward diffusion of MV^+ accompanying reduction of internal MV^{2+} was reversed upon transmembrane oxidation by $Fe(CN)_6^{3-}$, in effect restoring MV^{2+} to its original distribution before $S_2O_4^{2-}$ reduction.

b. Effects of Ionophores. The influence of several lipophilic cations and ion carriers upon transmembrane viologen migration and reaction stoichiometries and rates was investigated. The protonophores, carbonyl cyanide 3-chlorophenylhydrazone and 2,4-dinitrophenol, and the potassium-selective ionophore, valinomycin, which all act as uncouplers of oxidative phosphorylation in biological membranes,[30] were unable to facilitate transmembrane ion movement when added to suspensions of DHP membranes.[14] However, both the lipophilic tetraphenylphosphonium ion (TPP^+) and the *N*-methyl-4,4′-bipyridinium ion (MB^+), when added at concentrations approximately equal to the total viologen present, caused reduction of net inward MV^+ migration accompanying transmembrane MV^{2+} reduction to about 50% of the stoichiometric values measured in their absence. Vesicles that had accumulated high concentrations of MV^+ (by prior reduction with $S_2O_4^{2-}$ ion) rapidly leaked MV^+ when MB^+ was subsequently added to the medium; the equilibrium time was typically 3–5 min. The radical cation also leaked from DHP vesicles prepared in 75 mM imidazole buffer, pH 7.5, when lipophilic ions were not present. This effect is illustrated in Figure 3, where the initially formed MV^+ product, predominantly multimeric, converted to an equilibrium distribution containing the monomer as the major fraction. Addition of MB^+ accelerated this process. The imidazolium cation was, therefore, also apparently capable of dissipating the MV^+ gradient, albeit at a slower rate. In contrast, the initial multimer product spectrum was unchanged after 60 min when an analogous reaction was carried out in 20 mM Tris, pH 8.0, containing no added lipophilic ions.

The 1:1 stoichiometric correspondence of the extent of internal MV^{2+} reduction with the amount of external MV^{2+} initially

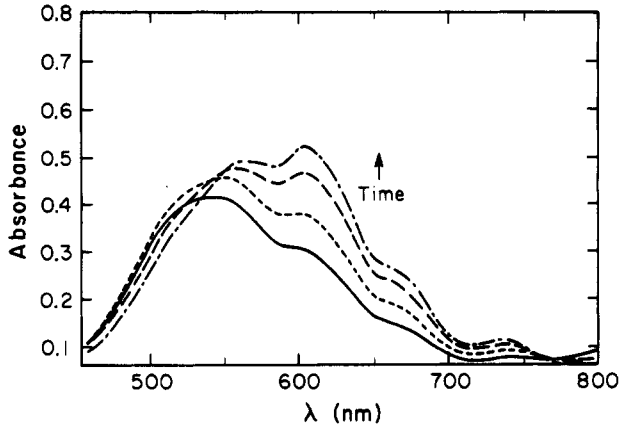

Figure 3. Optical spectra illustrating slow conversion of multimeric MV^+ radical cation to monomer following transmembrane reduction in imidazole buffer. Conditions: 4 mM DHP vesicles containing initially 34 μM internal and 25 μM external MV^{2+} in 75 mM imidazole-HCl, pH 7.5. Spectra were taken at 2, 5, 10 and 20 min following addition of $S_2O_4^{2-}$ ion. The absence of an isosbestic point is attributable to incomplete viologen reduction at the time that the initial spectrum was recorded.

TABLE II: Kinetics of Dithionite Reduction of DHP-Bound MV^{2+} Ions[a]

$[S_2O_4^{2-}]$ (mM)	$10^{-7}k_3$ (M^{-1} s^{-1})	$10^{-4}k_4$ (M^{-1} s^{-1})	
	A.[b-d] $[MV^{2+}]_i = [MV^{2+}]_o$		
12.5	0.28	1.3	1.3
20	0.41	0.7	1.9
30.5	0.60	2.1	1.2
35	0.70	1.6	1.1
40.5	0.80	2.0	1.6
26.5	0.50	1.4	1.6
26.5	1.5	[e]	1.7
29	0.56	1.8	0.7
35	0.57	2.0	0.7
35	1.2	[e]	0.7
	B.[b,f] $[MV^{2+}]_i \neq [MV^{2+}]_o$		
18, 24	1.1	1.2	1.2

[a] In 20 mM Tris-HCl, pH 8.0, at 23 °C. [b] Initial concentrations of MV^{2+} bound at the internal (i) and external (o) vesicle interfaces. [c] First five data entries [DHP] = 1 mM, all others [DHP] = 2 mM. [d] Determined from eq 3. [e] Too fast to measure. [f] Determined by computer simulation using the scheme given in Figure 5, where the relative contribution of the second pathway was negligible (<10%).

present that was observed under conditions where the internal concentration exceeded the external also changed when MB^+ ion was added to the bulk solution. For example, reduction of DHP vesicles in 20 mM Tris, pH 8.0, containing 32 μM internal MV^{2+} and 22 μM external MV^{2+} led to met formation of 42 μM MV^+, corresponding very closely to twice the initial external concentration. When 50 μM MB^+ was present, the same reaction gave complete reduction of all MV^{2+} present in the system. This effect was quite general and led to increased transmembrane reduction of MV^{2+} under a variety of conditions. We have previously demonstrated 1:1 membrane translocation of MB^+ per electron in a vectorially organized system for which this was the only lipophilic ion present in the external medium.[31]

c. Reaction Kinetics. Dithionite reduction of MV^{2+} that was equally distributed between the inner and outer DHP surfaces was clearly biphasic. Approximately one-half of the MV^{2+} was reduced in each of the steps, as measured by optical absorbance changes at 546 nm, the monomer/internal multimer isosbestic point. The first step was first-order in MV^{2+} and pseudo-first-order in SO^{2-} concentrations; the average calculated second-order rate constant was $k_3 = 1.6\ (\pm 0.4) \times 10^7\ M^{-1}\ s^{-1}$ (Table II). The slower reaction step could not be fit to one or two single-exponential functions but fit well to a homogeneous second-order rate law. The magnitude of the rate constant, $k_4 = 1.3\ (\pm 0.4) \times 10^4\ M^{-1}\ s^{-1}$, was independent of the $S_2O_4^{2-}$ concentration, which

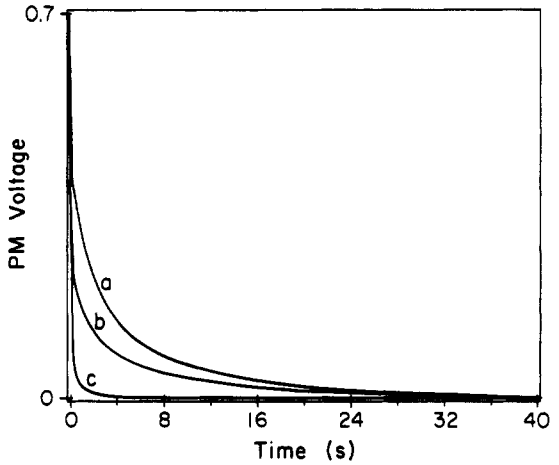

Figure 4. Wavelength dependence of kinetic waveforms for dithionite reduction of DHP-bound MV^{2+} ions. The time base was chosen to maximize temporal resolution of the outer and transmembrane reduction steps. Conditions: 4 mM DHP containing 49 μM inner and 35 μM outer MV^{2+} in 20 mM Tris-HCl, pH 8.0, 23 °C. (a) 520 nm, $2\epsilon_{monomer} = \epsilon_{multimer}$; (b) 546 nm, $\epsilon_{monomer} = \epsilon_{multimer}$; (c) 575 nm, $\epsilon_{monomer} = 2\epsilon_{multimer}$.

was varied over a 3-fold range (Table II). When the internal and external initial MV^{2+} concentrations were not identical, the simple bimolecular rate law for the second redox step was no longer valid. Under these conditions, the waveforms were simulated using a computer program that calculated incremental changes in the concentration of each species with time according to any postulated mechanism. With this program, the measured waveforms could be accurately reproduced at 546 nm using the rate law

$$d[MV^+]/dt = k_3[MV^{2+}]_o[SO^{2-}] + k_4[MV^+]_o[MV^{2+}]_i \quad (3)$$

assuming the rate constants k_3 and k_4 given above. In eq 3, the subscripts o and i refer to viologens bound at the vesicle outer and inner surfaces, respectively. When the initial MV^{2+} concentrations at both surfaces were the same, $[MV^+]_o = [MV^{2+}]_i$, and the second term becomes $k_4[MV^{2+}]_i^2$, accounting for the homogeneous second-order kinetics. A stepwise mechanism giving this rate law is illustrated graphically in Figure 5 as pathway a.

Dithionite titration of MV^{2+}–DHP vesicles established that the external MV^{2+} was reduced before the internal viologen. Initially only monomeric radical cation was formed, as determined spectroscopically, and no viologen redistribution was detected in oxygenation–reduction cycling experiments. Not until the $S_2O_4^{2-}$ reducing equivalents exceeded the initial external MV^{2+} concentration did multimeric MV^+ formation occur, which was accompanied by MV^+ radical cation uptake. These data, taken with the kinetic results, allow assignment of the fast and slow steps to reduction of the external and internal MV^{2+}, respectively.

Because the internally localized MV^+ was nearly entirely multimeric and the external MV^+ was monomeric, it was possible to use the wavelength dependence of the reaction to gain information about the relative rates of transmembrane reduction and aggregation of the internal MV^{2+} ion. Specifically, if aggregation were slow relative to the transmembrane redox step, the magnitude of k_4 would be wavelength dependent. Voltage–time waveforms, taken at several wavelengths, are displayed in Figure 4. The solid curve is the trace obtained at the isosbestic point, which is independent of absorbing species. Where the viologen radical chromophores in the monomer absorb twice as much as those in the multimer (575 nm, trace c), no change was observed following the fast reduction step. This result implies that transmembrane redox was rate-limiting since, if aggregation were slower, the transmittance would have increased with time over this interval. The third trace displayed (520 nm, trace a) was taken at a wavelength where the viologen radicals absorb twice as much in the multimer as in the monomer. The absorbance

TABLE III: Reaction Stoichiometry and Product Topographic Distributions in C_nMV^{2+}-Mediated Transmembrane Reduction of C_nMV^{2+} Ions[a]

n_i	$[C_nMV^{2+}]_i$[b] (μM)	n_o	$[C_nMV^{2+}]_o$[b] (μM)	$[C_nMV^+]/C_nMV^{2+}]_o$[c]	$\Delta[C_nMV^{2+}]_i$[d] (μM)
6	27	6	20	1.6	13
8	20	8	17	1.5	6.5
10	20	10	18	1.5	6.7
6	27	1	12	1.9	7.3
8	20	1	17	1.9	8.3
10	20	1	15	1.7	8.4
1	23	6	17	1.7	10.5
1	23	8	19	1.6	11
1	23	10	17	1.7	11
1	23	12	17	1.7	13
1	23	14	17	1.7	13
1	23	16	15	1.4	7

[a] Conditions: 1.5 mM DHP in 20 mM Tris-HCl, pH 8.0, 5-fold molar excess $S_2O_4^{2-}$ added. [b] Alkyl chain lengths (n) and initial concentrations of internally (i) and externally (o) bound C_nMV^{2+} ions. [c] Ratio of total viologen radical cations formed, determined spectrophotometrically, to initial amount of externally bound viologen. [d] C_nMV^{2+} ions accumulated after reduction–oxygenation cycling.

change corresponding to the slow step was twice that for the fast step, although the magnitude of k_4 was identical to values calculated at other wavelengths. This behavior established that multimer formation either coincided with, or rapidly followed, rate-limiting transmembrane reduction.

Transmembrane Reduction of C_nMV^{2+} Ions. *a. Reaction Stoichiometries.* Each of the viologens studied was capable of mediating transmembrane electron transfer to some degree, based upon the total amount of viologen reduced upon adding excess $S_2O_4^{2-}$ to the bulk medium. However, unlike the MV^{2+} ion, the stoichiometries were nonintegral and depended upon such factors as the viologen identity, the $[C_nMV^{2+}]$/DHP ratio, and, in some instances, the medium composition. Similarly, the extent of viologen aggregation at both interfaces and C_nMV^+ uptake per electron transferred across the bilayer varied with the C_nMV^{2+}–DHP composition and viologen alkyl chain length. Representative data are given in Table III. These experiments were made at low C_nMV^{2+}/DHP ratios, conditions which maximized differences between the C_nMV^{2+}–DHP and MV^{2+}–DHP stoichiometries. In general, for a given viologen, increasing the C_nMV^{2+}/DHP ratio caused both the extent of transmembrane reduction and net uptake of C_nMV^+ to increase, approaching limiting values equal to those measured for the MV^{2+}–DHP vesicles.

The extent of transmembrane reduction mediated by the long-chain analogs ($n \geq 12$) was uncertain because the internal and external concentrations could not be determined by the combined chromatographic–spectroscopic procedures used for the shorter-chain analogs. In asymmetrically organized vesicles containing encapsulated MV^{2+}, each of the C_nMV^{2+} ions was capable of mediating partial transmembrane reduction, although the extent of this reaction and $C_{16}MV^+$ uptake were particularly low for $C_{16}MV^{2+}$ (Table III). Viologen reduction by $S_2O_4^{2-}$ ion in DHP vesicles containing just $C_{16}MV^{2+}$ was also incomplete; at the highest $C_{16}MV^{2+}$/DHP ratios examined (0.018), only 78% reduction could be achieved in 20 mM Tris buffer. Assuming that, like the short-chain analogs, $C_{16}MV^{2+}$ adopted an inside:outside distribution of 1:2, this value corresponds to reduction of only one-third of the internally localized $C_{16}MV^{2+}$ ion. The extent of $C_{16}MV^+$ radical ion uptake was also low, based upon changes in the relative amplitudes of fast and slow components in the kinetic traces for reduction by $S_2O_4^{2-}$ ion following reduction–oxygenation cycling. For $C_{16}MV^{2+}$–DHP vesicles, these changes indicated only 0.2–0.3 $C_{16}MV^+$ ions were taken up per cycle. However, when MV^{2+} or MB^+ was added to a partially reduced vesicle suspension containing $S_2O_4^{2-}$ ion, additional $C_{16}MV^{2+}$ was reduced by an amount that coincided with the amount of added cation; with MV^{2+} or MB^+ in excess, complete reduction of $C_{16}MV^{2+}$ to the radical cation was achieved. Reduction also went to completion when $C_{16}MV^{2+}$–DHP vesicles were reacted with $S_2O_4^{2-}$ ion in 75 mM imidazole, pH 7.5.

b. Reaction Kinetics. Dithionite reduction of DHP-bound C_6MV^{2+}, $C_{12}MV^{2+}$, and $C_{16}MV^{2+}$ ions was examined quantitatively. As with MV^{2+}, DHP vesicles were prepared with equal quantities of C_6MV^{2+} on both sides of the vesicle bilayer. The data fit well the rate law given by eq 3. The value for $k_3 = 1.0\ (\pm 0.12) \times 10^7\ M^{-1}\ s^{-1}$ in 20 mM Tris, pH 8.0, was identical to the rate constant determined for reduction of C_6MV^{2+} bound only to the external surface of DHP under identical conditions, i.e., $k_1' = 1.2\ (\pm 0.2) \times 10^7\ M^{-1}\ s^{-1}$.[7] This rate constant was independent of the viologen-to-surfactant molar ratio, varied over the range C_6MV^{2+}/DHP = 0.011–0.032. The slow step, k_4, was independent of $S_2O_4^{2-}$ ion concentration over a 10-fold range but appeared to increase slightly with increasing C_6MV^{2+}/DHP ratios (r); in three separate sets of experiments with r values averaging 0.015, 0.026, and 0.027, rate constants $k_4 = 1.1\ (\pm 0.2) \times 10^3$, $1.6\ (\pm 0.6) \times 10^3$, and $3.3\ (\pm 0.3) \times 10^3\ M^{-1}\ s^{-1}$, respectively, were obtained. Amplitudes of the two steps were approximately equal at the isosbestic point, and the rate constants were independent of the monitoring wavelength, again implying that the aggregation accompanying C_6MV^+ uptake by the vesicle coincided with or rapidly followed rate-limiting transmembrane reduction of the C_6MV^{2+} ion.

Two problems were encountered in studying the reaction dynamics of DHP vesicles containing the long-chain C_nMV^{2+} ion, both of which were solved by replacing the medium with 75 mM imidazole, pH 7.5. One problem, discussed in the preceding section for $C_{16}MV^{2+}$ ion, was that the extent of transmembrane reduction was severely limited in Tris buffers. The other was that the C_nMV^+ radical ions underwent slow decomposition, both in aqueous solution and when DHP-bound, yielding a green fluorescent compound with a major emission peak at 520–524 nm.[14] Similar compounds have previously been observed in various decomposition and oxidation reactions involving viologen radicals.[32-34] They have tentatively been identified as pyridones, based upon their spectral properties. The C_nMV^+ decomposition rates increased with increasing viologen alkyl chain lengths and were sensitive to the medium buffer identity and ionic strengths. This side reaction was generally not a problem but was found to distort the tail of the kinetic curve for $C_{16}MV^{2+}$ reduction in Tris buffers. This ion exhibited both the fastest decomposition and slowest transmembrane oxidation–reduction rates. Several alternative buffers were found for which radical ion decomposition was considerably attenuated.[14] Imidazole, at 75 mM and pH 7.5, was ultimately chosen because this medium simultaneously retarded the decomposition rate and provided sufficient vesicle stability to allow the kinetic measurements.

The reaction dynamics were analyzed by computer simulation assuming that two kinetically distinct reaction environments existed within the vesicles, as implied by the observations that $S_2O_4^{2-}$ reduction of the externally bound C_nMV^{2+} ions was biphasic (eq 2) and that only partial reduction of internal C_nMV^{2+} ions occurred in Tris-buffered solutions. A schematic diagram

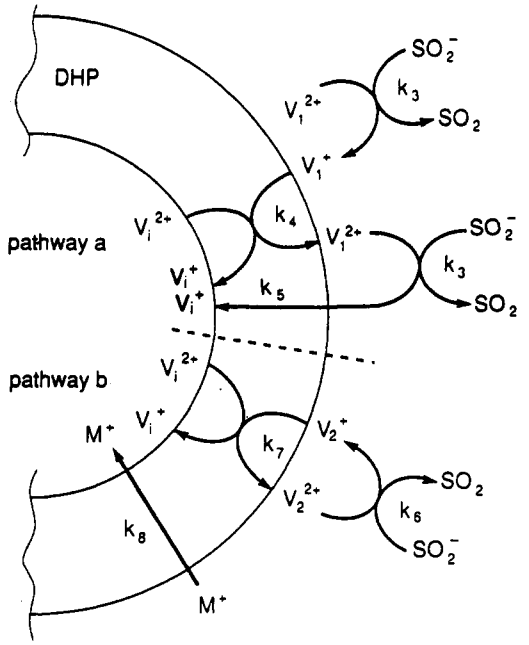

Figure 5. General kinetic scheme for C_nMV^{2+}-mediated transmembrane reduction of C_nMV^{2+} ions. Two separate pathways are included to accommodate observations that, for the long-chain ($n \geq 12$) analogs, two kinetically distinguishable binding domains were detectable and internal reduction was incomplete unless lipophilic ions were added to the medium.

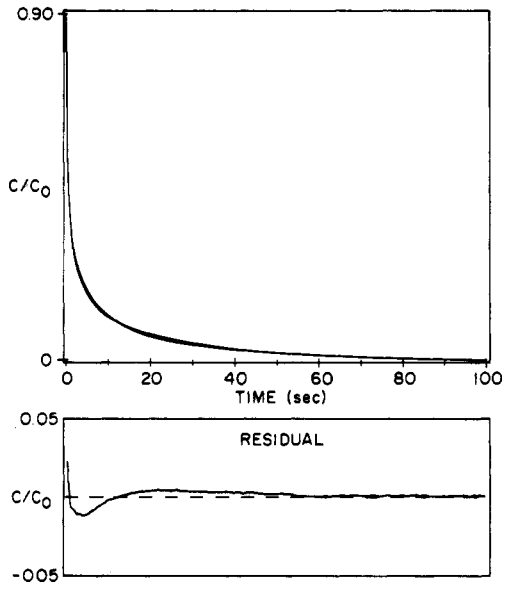

Figure 6. Kinetic waveforms and computer-simulated fit for dithionite reduction of $C_{12}MV^{2+}$–DHP. Conditions: 0.44 mM $S_2O_4^{2-}$ added to 2 mM DHP containing 81 μM $C_{12}MV^{2+}$ in 75 mM imidazole-HCl, pH 7.5. The kinetic scheme given in Figure 5 was used for the simulation assuming equal contributions from the two pathways and rate constants $k_3 = 6.2 \times 10^6$ M^{-1} s^{-1}, $k_4 = 4.0 \times 10^2$ M^{-1} s^{-1}, $k_6 = 1.3 \times 10^6$ M^{-1} s^{-1}, and $k_7 = 8.0 \times 10^3$ M^{-1} s^{-1}.

of the reaction sequence is given in Figure 5. Representative fits of the voltage–time waveforms obtained are given in Figures 6 and 7 for $C_{12}MV^{2+}$–DHP and $C_{16}MV^{2+}$–DHP, respectively. An initial inside:outside equilibrium distribution of C_nMV^{2+} of 1:2 was assumed. The kinetic curves were not affected by adding MB^+ or MV^+ to the medium, implying the transmembrane diffusion of lipophilic ions (k_5 and k_8, Figure 5) was rapid relative to the transmembrane redox steps (k_4 and k_7, Figure 5). These were modeled as bimolecular processes according to eq 3. The relative proportion of reaction by the two pathways and the rate constants for SO^{2-} reduction of externally bound C_nMV^{2+} ions (k_3 and k_6, Figure 5) were adjusted to give reasonable data fits. The latter provide a check on the validity of the simulation method

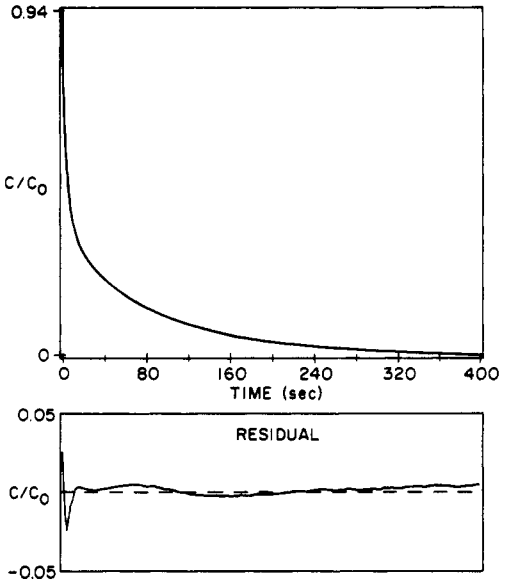

Figure 7. Kinetic waveform and computer-simulated fit for dithionite reduction of $C_{16}MV^{2+}$–DHP. Conditions: 1.3 mM $S_2O_4^{2-}$ added to 2 mM DHP containing 75 μm $C_{16}MV^{2+}$ in 75 mM imidazole-HCl, pH 7.5. The kinetic scheme from Figure 5 was used for the simulation assuming 30% contribution from pathway a and rate constants $k_3 = 1.0 \times 10^6$ M^{-1} s^{-1}, $k_4 = 2.0 \times 10^2$ M^{-1} s^{-1}, $k_6 = 1.2 \times 10^5$ M^{-1} s^{-1}, and $k_7 = 4.0 \times 10^3$ M^{-1} s^{-1}.

since, based upon comparison with the short-chain analogs, these rate constants should be very similar to the k_1' and k_2' values measured for reduction of C_nMV^{2+} ions bound only to external DHP surfaces. Best fit values for $C_{12}MV^{2+}$–DHP were $k_5 = 5.5$ ($\pm$0.7) $\times 10^6$ M^{-1} s^{-1} and $k_6 = 1.2$ ($\pm$0.1) $\times 10^6$ M^{-1} s^{-1} and, for $C_{16}MV^{2+}$–DHP, were $k_5 = 1.0$ ($\pm$0.2) $\times 10^6$ M^{-1} s^{-1} and $k_6 = 0.2$ ($\pm$0.04) $\times 10^6$ M^{-1} s^{-1}, which were nearly identical to the values for k_1' and k_2' reported above. Second-order rate constants for transmembrane reduction and approximate relative contributions of each pathway to the overall reaction for all the reactions studied are collected in Table IV. In general, the fits were very sensitive to the values taken for the reaction parameters; measurable changes occurred in the statistical parameter (χ^2) and, visually, in the residual plots (Figures 6 and 7) when individual rate constants or relative amplitudes of the pathways were changed by 10%. Rate constants measured for $C_{12}MV^{2+}$–DHP and $C_{16}MV^{2+}$–DHP reduction were independent of $S_2O_4^{2-}$ concentration over a 6-fold range.

Discussion

Reaction Pathways. Two distinct transmembrane redox pathways can be identified, based upon whether or not net inward translocation of external C_nMV+ occurs. As exemplified by MV^{2+}–DHP vesicles, the "diffusional" pathway involves 1:1 stoichiometric uptake of the viologen radical cation per electron transferred (Figure 5, pathway a). In the other, "electron-transfer" pathway, the viologen radical cation cannot penetrate the bilayer and appreciable transmembrane redox occurs only if additional membrane-permeable ions are present to comigrate with the electron (Figure 5, pathway b). Both pathways are apparently expressed simultaneously in several C_nMV^{2+}–DHP systems; for the most extensively studied of these, $C_{16}MV^{2+}$–DHP, the electron-transfer pathway predominated by about a 2:1 ratio. These results differ from an earlier cursory study of transmembrane redox in Tris buffers,[7] from which it was concluded that transmembrane reduction of the short-chain C_nMV^{2+} ions ($n \leq 10$) did not occur and that, for the long-chain analogs, the rate was half-order in $S_2O_4^{2-}$ ion. In the earlier work, nearly all of the kinetic data were taken at wavelengths near the radical cation monomer absorption maxima, a condition

which made detection of the transmembrane redox step difficult (Figure 4, trace c).

The kinetic models presented in Figure 5 can, at least qualitatively, account for the dynamical properties exhibited by the C_nMV^{2+} ions. Thus, in all cases (i) rate laws for reduction of externally bound C_nMV^{2+} coincided with the fast components of reduction observed when viologen was bound at both interfaces, (ii) the slow steps were independent of reductant concentration and identity, consistent with a transmembrane redox process, and (iii) the relative amplitudes of the two steps corresponded to known or anticipated relative proportions of externally and internally localized C_nMV^{2+} ions. In the models, transmembrane electron transfer is electrogenic and, in the absence of charge-compensating ion movement, would quickly polarize the membrane, generating a potential that opposed further reaction.[1a] For systems in which the radical cations are membrane-permeable, e.g., MV^+, ion uptake would be driven by the potential, which is negative inside, until either the external medium was depleted of radical cation or the reaction reached completion. In instances where the radical cation was not membrane-permeable, e.g., reaction pathway b for $C_{16}MV^+$, transmembrane reduction would be blocked by the unfavorable potential unless lipophilic cations were added that could diffuse across the DHP membrane and dissipate the potential. In these cases, stoichiometric uptake of the lipophilic ion would occur, as was observed. In reactions where viologen radical cation translocation occurred, competitive uptake by added lipophilic ions would reduce the extent of C_nMV^+ uptake. Lowered stoichiometric ratios of C_nMV^+ ions accumulated per internal C_nMV^{2+} ions reduced would also occur in instances where electrolyte diffusion competed for radical cation diffusion, e.g., as observed for reactions in media containing imidazolium ion.

Several additional observations can be rationalized in terms of this apparent tight coupling between the primary transmembrane redox reaction and charge-compensating ion movement. First, the absence of net MV^+ ion uptake in anaerobic reduction–oxidation cycling with $S_2O_4^{2-}$ and $Fe(CN)_6^{3-}$ ions arose by reversible uptake and release of C_nMV^+ ions. Following the reduction half-cycle, spectroscopic determination of the relative extent of multimer formation established that MV^+ translocation had occurred; upon reoxidation, the original distribution was restored. Because $Fe(CN)_6^{3-}$ is membrane impermeable,[6,17] MV^+ oxidation required outward electron transfer, polarizing the membrane in the opposite sense as reduction and driving MV^+ ion efflux. Similarly, the enhanced uptake of the short-chain C_nMV^{2+} ions accompanying oxygenation of vesicle suspensions at high $S_2O_4^{2-}$ concentration levels can be attributed to more rapid net oxidation of the viologen radicals in the vesicle interior, which was devoid of reductant. Under these circumstances, additional inward transmembrane redox would be favored, leading to additional C_nMV^+ uptake, because the intermediary level of oxidation inside the vesicles was greater than outside. The relative contribution by the "pumping" process would be expected to increase with the time required to complete O_2 oxidation of the system, which increased with increasing concentrations of excess $S_2O_4^{2-}$ ion present in the system. Finally, introduction of a second lipophilic ion will collapse by coupled antiport the concentration gradients that were generated by ion uptake in the primary transmembrane redox process, e.g., as was observed for MV^+-containing vesicles in imidazole buffers (Figure 3).

The central premise of the kinetic model—that C_nMV^{2+} ions are membrane-impermeable and, therefore, that the reaction dynamics are dictated by the permeabilities of the viologen radical cations or other species—has been confirmed for several reactants by direct measurement of passive diffusion rates using ^{14}C-labeled viologens.[11] In these studies, no exchange of radiolabel between the internal and external pools of C_nMV^{2+} ions (n = 1, 6, 12, 16) occurred within 30 h, although rapid exchange was observed when the external pools were partially reduced. Remarkably, for $C_{16}MV^{2+}$ ion, this exchange proceeded only about one-third toward equilibrium, indicating that the major fraction of the amphiphile was in a nonexchangeable environment, i.e., could not traverse the bilayer. For the exchanging ions, rate constants decreased in the order $MV^+ \simeq C_6MV^+ > C_{12}MV^+ \simeq C_{16}MV^+$.

TABLE IV: Transmembrane Oxidation–Reduction Rate Constants[a]

viologen	medium	k (M^{-1} s^{-1})[b]	pathway percentage
MV^{2+}	20 mM Tris-HCl, pH 8.0	$k_4 = 1.3 \times 10^4$	~100
C_6MV^{2+}	20 mM Tris-HCl, pH 8.0	$k_4 = 1.6 \times 10^3$	~100
$C_{12}MV^{2+}$	75 mM imidazole, pH 7.5	$k_4 = 7 \times 10^1$	~50
		$k_7 = 6 \times 10^3$	~50
$C_{16}MV^{2+}$	75 mM imidazole, pH 7.5	$k_4 = 1 \times 10^2$	~35
		$k_7 = 7 \times 10^2$	~65

[a] [DHP] = 1–2 mM, 23 °C. [b] Rate constants defined by the reaction scheme given in Figure 5.

Molecular Mechanisms. *Electron Transfer.* Although two transmembrane oxidation–reduction pathways can be readily identified from the transverse diffusional properties of the viologen radical cations, the molecular details of the reactions are less apparent. The macroscopic properties of DHP vesicles containing C_nMV^{2+} ions gave no evidence of particle heterogeneity when examined by dynamic light scattering and freeze–fracture electron microscopy.[3] Hence, the heterogeneity that is evident from C_nMV^{2+}–DHP reactions with aqueous-phase reductants and the simultaneous formation of monomeric and multimeric forms of C_nMV^+ must be microscopic in origin. On the basis of data mentioned in the Introduction, we had previously proposed that the C_nMV^{2+} ions could either bind at the vesicle aqueous–hydrocarbon interface or interpenetrate the bilayer, the distribution being governed by the pendant alkyl chain length. Accordingly, electron transfer was thought to occur with the long-chain analogs because interpenetration both reduced the transverse diffusion rates of the C_nMV^+ ions and reduced the electron tunneling distance to one-half of the bilayer width, a distance consistent with the measured rate constants.[1a] This interpretation is not unique, however. A second possibility is that the pathways involving the monomeric and aggregated forms are different. Specifically, we have found that a covalently linked diviologen diradical cation (1,1″-propanediylbis(1-methyl-4,4′-bipyridinium), PMV^{2+}) is unable to traverse the DHP bilayer[14] (Lymar, S. V., Newell, K. L., unpublished observations), and other studies[35] involving simultaneous spectroscopic and electrochemical measurements to locate MV^+ ions in DHP vesicular systems have suggested that the multimeric form of MV^+ is also membrane-impermeable. The optical spectrum of the reduced PMV^{2+} diradical cation in DHP indicated essentially complete formation of the multimer. The same spectral features were observed in aqueous solution and have been attributed to intramolecular dimerization characterization by π-stacking of the bipyridine rings.[36] Assuming these dynamical properties are general, we would identify the increasing relative contribution of the electron-transfer pathways as the C_nMV^{2+} alkyl chain lengthened to an increasing proportion of membrane-impermeable multimeric form. This model is capable of rationalizing the otherwise puzzling observation that, although apparently second order, the transmembrane rate constants were insensitive to the degree of surface coverage by the C_nMV^{2+} ions. The rate constants were calculated using analytically determined bulk solution concentrations of the viologens. This procedure ignored the fact that effective interfacial concentrations depend upon the C_nMV^{2+}/DHP ratios. Varying these ratios over a 4-fold range only increased the apparent bimolecular rate constants by about 50% in the several systems investigated. Since this variation was within experimental uncertainty, the data reported in Table IV are averaged values. If the viologens were distributed between isolated monomers and

laterally phase-separated domains, increasing the total coverage might not increase significantly either the monomer concentration or number of domains within the vesicle and could, therefore, have minimal effect upon the transmembrane redox dynamics. This type of partitioning between monomers and aggregate "islands" in vesicles has been described for other amphiphilic dopants with similar structural features.[10,37]

A distinguishing characteristic of this pathway is that transmembrane reduction of viologens does not occur unless lipophilic ions are added to the medium. Assignment of an electron-transfer mechanism to this pathway rests on the premise that the lipophilic ions are redox-inactive. For imidazole/imidazolium ion buffers, this is almost certainly the case since reduction of this species in aqueous solution has never been observed; reported studies include electrochemical analyses to −1.2 V vs NHE.[38] However, the standard one-electron reduction potential for MB^+ is $E^{0\prime}(MB^{+/0}) = -0.87$ V under the experimental conditions[39] so that, in the presence of $S_2O_4^{2-}$ ion, about 0.01% of this species was reduced to the neutral radical. Although minuscule, this concentration level could be sufficiently high for MB^0 to act as a membrane-permeable intermediary reductant, in effect short-circuiting electron transfer between C_nMV^{2+} and C_nMV^+ ions by diffusing across the bilayer and directly reducing the internal C_nMV^+ ions in an electroneutral reaction. Consistent with this possibility, the intrinsic rate constant for passive diffusion of the structurally similar MV^+ radical cation across DHP SUV bilayers is $k_p = 4 \times 10^{-2}$ s^{-1}, which is 10^2–10^4-fold slower than expected for comparable uncharged radicals.[11] Thus, although MB^0 was present at only 0.01% of the total added MB^+, its flux through the bilayer could equal or exceed that of the cation. Ongoing studies in our laboratory involving measurement of MB^+ transmembrane diffusion rates and MB^+-mediated transmembrane reduction of PMB^{4+} ion also support a mechanism in which MB^0 is a membrane-permeable redox carrier (Lymar, S. V.; Newell, K. L., unpublished observations).

Transmembrane Diffusion. Identifying the molecular mechanism for pathways involving net translocation of C_nMV^+ has proved difficult because the DHP-bound radical cations disproportionate to some extent,[4] i.e.

$$2C_nMV^+ \rightleftharpoons C_nMV^0 + C_nMV^{2+} \qquad (4)$$

It is possible that the actual transmembrane redox carrier is C_nMV^0 which, in effect, shuttles the electron and C_nMV^+ as a single entity. Three possible mechanisms are illustrated in Figure 8. Scheme a involves transmembrane electron transfer followed by MV^+ migration, scheme b involves simple C_nMV^0 diffusion, and scheme c considers the possibility that both C_nMV^0 and C_nMV^+ can act as diffusing elements, thereby establishing a transmembrane electron shuttle.

In scheme a, electron transfer is depicted as being facilitated by a transitory mixed-valent MV^{2+}–MV^+ intermediate which undergoes one-electron reduction by $S_2O_4^{2-}$ in the bulk solution, forming directly the purple $(MV^+)_2$ dimer. Reasons for proposing this type of intermediate are (i) simple diffusion of C_nMV^+ across the bilayer does not lead to net transmembrane oxidation–reduction and (ii) electron tunneling probabilities across the full hydrocarbon bilayer width (~40 Å)[3] are prohibitively low,[1a] so that some barrier penetration is essential. The purple coloration of DHP-encapsulated MV^+ ions is indicative of "pimerization" or planar π-overlap of the heterocyclic rings.[36,40-42] Such configurations might be most easily achieved if the MV^+ ions were collinear with the surfactant molecules in the inner bilayer leaflet. This binding geometry would facilitate formation of a bilayer-spanning aggregate. The hypothetical species envisioned is similar to other transverse dimers proposed from kinetic evidence to form bilayer-spanning electron-conducting channels;[43,44] a precedent for its existence is suggested from the electrochemical properties of the *N*-ethyl-*N*-(trimethylamino)-4,4′-bipyridinium

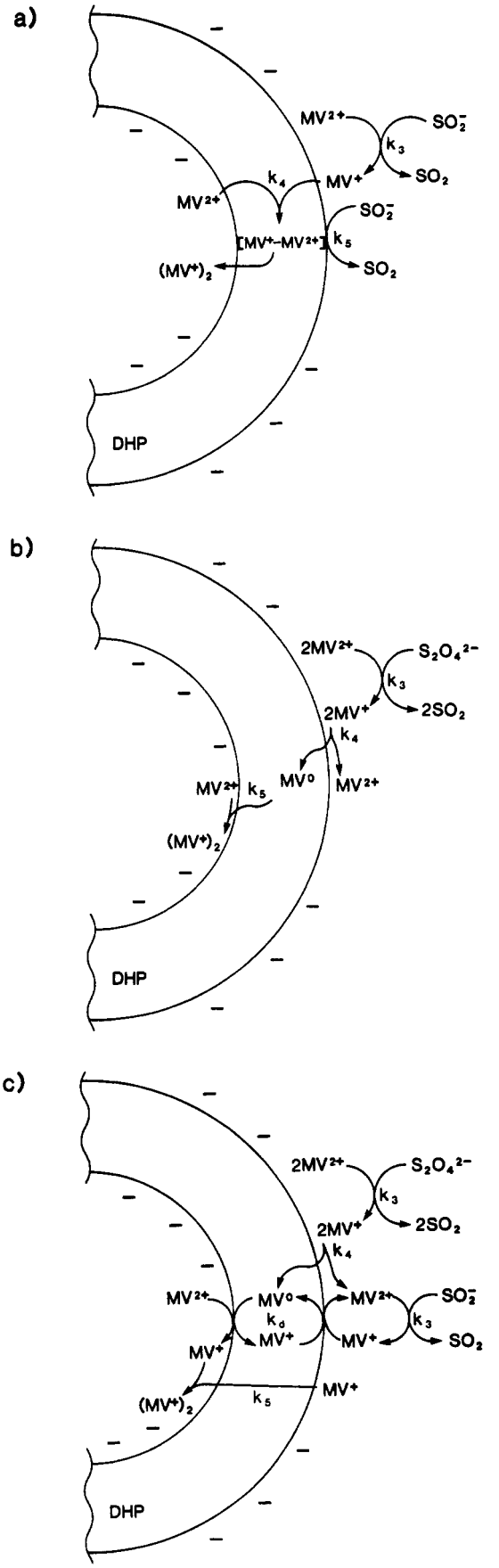

Figure 8. Alternative mechanisms for the "diffusional" pathway. Pathway a: transmembrane reduction of MV^{2+} by MV^+; formation of a membrane-localized mixed-valent intermediate is proposed to account for re-reduction of the electron donor by $S_2O_4^{2-}$ ion in the bulk aqueous phase. Pathway b: transmembrane diffusion of MV^0. Pathway c: diffusion of both MV^0 and MV^+, forming a transmembrane electron shuttle. To account for the observed rate law, the k_4 step must be rate limiting in all cases.

ion, which was reported to undergo sequential 0.5- and 1.5-electron-transfer steps in the course of reduction to V^0.[45] Also, two-electron reduction of PMB^{4+} and related tetraquaternary bipyridinium ions capable of intramolecular dimerization proceeded in one-electron steps.[46] The potentials for formation of radical trications and diradical dications were separated by about 150 mV, indicating stabilization of the intermediate oxidation state by intramolecular V^{2+}–V^+ complexation.

We had tentatively excluded mechanisms b and c on the basis that they predict a transmembrane redox rate constant that is $S_2O_4^{2-}$-dependent, but no dependence upon reductant could be established experimentally.[1a,47] This dependence arises because, under our experimental conditions where C_nMV^0 does not accumulate, the steady-state levels of C_nMV^0 should be determined by the redox poise of the system, which was governed by the $[SO^{2-}]/[SO_3^{2-}]$ ratio. However, if C_nMV^+ disproportionation were rate-limiting, rather than C_nMV^0 transmembrane diffusion, the predicted rate law for mechanisms b and c would be second order in $[C_nMV^+]_0$ and independent of $S_2O_4^{2-}$ ion concentrations, i.e., identical to eq 3 when initial C_nMV^{2+} concentrations at the inner and outer interfaces were equal. The apparent mixed second-order rate law observed for other C_nMV^{2+} ion distributions (eq 3) cannot be rationalized by these mechanisms, but given the complexity of these reactions, it is difficult to establish unique rate laws based upon quantitative fits of simulated curves. A lower limit for the C_nMV^0 formation rate constant (k_f) estimated from the disproportionation equilibrium constant, $K = k_f/k_r = 6 \times 10^{-6}$ (eq 4)[24] assuming that the reverse rate constant is diffusion controlled, i.e., $k_r \leq 10^{10}\ M^{-1}\ s^{-1}$, is $k_r \leq 6 \times 10^4\ M^{-1}\ s^{-1}$. Since the rate of diffusion at the DHP interface is probably lower than in aqueous solution, the actual value of k_f might be considerably less than this limit. In any event, the estimated value is the same order of magnitude as the net transmembrane redox rate constants listed in Table IV, indicating the plausibility of rate-limiting C_nMV^0 formation. Evidence supporting $C_{16}MV^0$ as the redox carrier in transmembrane redox reactions across phosphatidylcholine vesicle bilayer membranes has recently been reported.[48]

It is also instructive to examine whether C_nMV^+ transmembrane diffusion rates could support mechanisms a and c. The diffusion constant for MV^+ and C_6MV^+ ions is $k_p = 4 \times 10^{-2}\ s^{-1}$.[11] The diffusion rate will be accelerated in mechanism a by the membrane potential ($\Delta\psi$), which develops as a consequence of electrogenic transmembrane reduction of the internal MV^{2+} ion. The maximum attainable value for $\Delta\psi$ is given by the thermodynamic driving force for the transmembrane reaction; for $S_2O_4^{2-}$ reduction of C_6MV^{2+}–DHP, $\Delta E \simeq 220\ mV \geq \Delta\psi$.[4,24] Assuming a symmetrical barrier, the inward diffusion rate constant (k_i) is $k_p \leq k_i \leq k_p e^{F\Delta\psi/2RT} \simeq 0.04\text{–}2.8\ s^{-1}$, where F is Faraday's constant. For mechanism c, membrane polarization is negligible and k_p is the appropriate rate constant. The corresponding limiting reaction half-times, $t_{1/2} = 0.2\text{–}17$ s, are the same order of magnitude as the apparent reaction half-times for transmembrane oxidation–reduction (cf. Figure 4). Therefore, both mechanisms appear to meet this kinetic criterion; i.e., if the estimated diffusion rates were much lower than the redox rates, the mechanisms could not have accounted for the rate behavior.

Irrespective of the actual mechanism, the decreasing order of relative rate constants from $MV^{2+} > C_6MV^{2+} > C_{16}MV^{2+}$ (Table IV) is consistent with the rate-limiting step containing a strong diffusional component. The slower of the two transmembrane reduction steps for $C_{12}MV^{2+}$–DHP also fits this progression. This order of relative rates is the same as for passive diffusion of the radical cations.[11] However, the redox rates spanned a range of 10^2-fold, whereas the range for diffusion was less than 10-fold.

Conclusions. Two distinct pathways have been identified for transmembrane oxidation–reduction reactions between DHP vesicle-bound C_nMV^{2+} and C_nMV^+ ions. One pathway necessarily involves electron transfer because the reactants cannot diffuse across the bilayer on the reaction time scale; the other is diffusional in the sense that transmembrane redox is accompanied by net transmembrane migration of C_nMV^+ ions. This kinetic model is supported by direct measurements of redox rates and topographic redistributions of viologens following reaction, the influence of lipophilic ions upon reactivities and, in separately reported studies,[11] intrinsic permeabilities of the viologens. Expression of either pathway appears to depend upon the supramolecular organization of the viologens within the membrane bilayer. For the "diffusional" pathway, identification of the actual diffusing species, C_nMV^0 or C_nMV^+, will require additional studies on diffusion dynamics, which are in progress.

Acknowledgment. Funding for this research was provided by the Office of Basic Energy Sciences, U.S. Department of Energy, under Grant DE-FG 87ER 13664.

References and Notes

(1) Recent reviews include: (a) Hurst, J. K. In *Kinetics and Catalysis in Microheterogeneous Systems*; Surfactant Science Series Vol. 38; Marcel Dekker: New York, 1991; pp 183–226. (b) Lymar, S. V.; Parmon, V. N.; Zamaraev, K. I. In *Photoinduced Electron Transfer III*; Topics in Current Chemistry, Vol. 159; Springer-Verlag: Berlin, 1991; pp 1–66. (c) Robinson, J. N.; Cole-Hamilton, D. J. *Chem. Soc. Rev.* **1991**, *20*, 49–94.

(2) Persuasive arguments for involvement of long-range electron transfer have been advanced in the transmembrane reduction of a phosphatidylcholine analog containing an isoalloxazine ring covalently attached to its β-alkyl chain near the surfactant headgroup. Tabushi, I.; Hamachi, I.; Kobuke, Y. *J. Chem. Soc., Perkin Trans. 1* **1989**, 383–390.

(3) Humphry-Baker, R.; Thompson, D. H.; Lei, Y.; Hope, M. J.; Hurst, J. K. *Langmuir* **1991**, *7*, 2592–2601.

(4) Lei, Y.; Hurst, J. K. *J. Phys. Chem.* **1991**, *95*, 7918–7925.

(5) Colaneri, M. J.; Kevan, L.; Thompson, D. H.; Hurst, J. K. *J. Phys. Chem.* **1987**, *91*, 4072–4077.

(6) Hurst, J. K.; Lee, L. Y. C.; Grätzel, M. *J. Am. Chem. Soc.* **1983**, *105*, 7048–7056.

(7) Thompson, D. H. P.; Barrette, W. C., Jr.; Hurst, J. K. *J. Am. Chem. Soc.* **1987**, *109*, 2003–2009.

(8) Hurst, J. K.; Thompson, D. H. P. *Inorg. Chem.* **1987**, *26*, 39–43.

(9) Hurst, J. K.; Thompson, D. H. P.; Connolly, J. S. *J. Am. Chem. Soc.* **1987**, *109*, 507–515.

(10) Yamazaki, I.; Tamai, N.; Yamazaki, T. *J. Phys. Chem.* **1990**, *94*, 516–525.

(11) Lymar, S. V.; Hurst, J. K. *J. Am. Chem. Soc.* **1992**, *114*, 9498–9503.

(12) Creutz, C.; Sutin, N. *Inorg. Chem.* **1974**, *13*, 2041–2043.

(13) Petitou, M.; Tuy, F.; Rosenfeld, C. *Anal. Biochem.* **1978**, *91*, 350–353.

(14) Patterson, B. C. Ph.D. Dissertation, Oregon Graduate Institute of Science and Technology, 1990.

(15) Norton, K. A., Jr.; Hurst, J. K. *J. Am. Chem. Soc.* **1978**, *100*, 7237–7242.

(16) Bevington, P. R. In *Data Reduction and Error Analysis for the Physical Sciences*; McGraw-Hill; New York, 1969.

(17) Lee, L. Y. C. Ph.D. Dissertation, Oregon Graduate Center, 1985.

(18) McLaughlin, S. *Curr. Top. Membr. Transp.* **1977**, *9*, 71–144.

(19) Lukac, S.; Harbour, J. R. *J. Am. Chem. Soc.* **1983**, *105*, 4248–4250.

(20) Maidan, R.; Goren, Z.; Becker, J. Y.; Willner, I. *J. Am. Chem. Soc.* **1984**, *106*, 6217–6222.

(21) Tabushui, I.; Kugimiya, S. *Tetrahedron Lett.* **1984**, *25*, 3723–3726.

(22) Brugger, P.-A.; Infelta, P. P.; Braun, A. M.; Grätzel, M. *J. Am. Chem. Soc.* **1981**, *103*, 320–326.

(23) Hoshino, K.; Sasaki, H.; Suga, K.; Sagi, T. *Bull. Chem. Soc. Jpn.* **1987**, *60*, 1521–1522.

(24) Mayhew, S. G. *Eur. J. Biochem.* **1978**, *85*, 535–547.

(25) Watanabe, T.; Honda, K. *J. Phys. Chem.* **1982**, *86*, 2617–2619.

(26) Tsukuhara, K.; Wilkins, R. G. *J. Am. Chem. Soc.* **1985**, *107*, 2632–2635.

(27) Lambeth, D. O.; Palmer, G. *J. Biol. Chem.* **1973**, *248*, 6095–6103.

(28) Patterson, B. C.; Thompson, D. H.; Hurst, J. K. *J. Am. Chem. Soc.* **1988**, *110*, 3656–3657.

(29) Oliviera, L. A. A.; Haim, A. *J. Am. Chem. Soc.* **1982**, *104*, 3363–3366.

(30) See, e.g.: Harold, F. M. *The Vital Force: A Study of Bioenergetics*; W. H. Freeman: New York, 1986.

(31) Patterson, B. C.; Hurst, J. K. *J. Chem. Soc., Chem. Commun.* **1990**, 1137–1138.

(32) Mau, A. W.-H.; Overbeek, J. M.; Loder, J. W.; Sasse, W. H. F. *J. Chem. Soc., Faraday Trans. 2* **1986**, *82*, 869–876.

(33) McKellar, J. F.; Turner, P. H. *Photochem. Photobiol.* **1971**, *13*, 437–440.

(34) Shelepin, I. V.; Barachevskii, V. A.; Kunavin, N. I. *Russ. J. Phys. Chem.* **1975**, *49*, 1019–1021.

(35) Tricot, Y.-M.; Manassen, J. *J. Phys Chem.* **1988**, *92*, 5239–5244.
(36) Furue, M.; Nozakura, S. *Bull. Chem. Soc. Jpn.* **1982**, *55*, 513–516.
(37) Kunitake, T.; Ihara, H.; Okahata, Y. *J. Am. Chem. Soc.* **1983**, *105*, 6070–6078.
(38) Elving, P. J.; Pace, S. J.; O'Reilly, J. E. *J. Am. Chem. Soc.* **1973**, *95*, 647–658.
(39) Harriman, A.; Millward, G. R.; Neta, P.; Richoux, M. C.; Thomas, J. M. *J. Phys. Chem.* **1988**, *92*, 1286–1290.
(40) Poizat, O.; Sourisseau, C.; Giannotti, C. *Chem. Phys. Lett.* **1985**, *122*, 129–132.
(41) Bockman, T. M.; Kochi, J. K. *J. Org. Chem.* **1990**, *55*, 4127–4135.
(42) Geuder, W.; Huenig, S.; Suchy, A. *Tetrahedron* **1986**, *42*, 1665–1677.
(43) Tabushi, I.; Nishiya, T.; Shimomura, M.; Kunitake, T.; Inokuchi, H.; Tatsuhiko, K. *J. Am. Chem. Soc.* **1984**, *106*, 219–226.
(44) Yusopov, R. G.; Asanov, A. N.; Khairutdinov, R. F. *Izv. Akad. Nauk SSSR Ser. Khim.* **1985**, 277–282.
(45) Porat, Z.; Zinger, B.; Tricot, Y. M.; Rubinstein, I. *J. Electrochem. Soc.* **1990**, *137*, 157C.
(46) Attalla, M. I.; McAlpine, N. S.; Summers, L. A. *Z. Naturforsch.* **1984**, *396*, 74–78.
(47) Patterson, B. C.; Thompson, D. H.; Hurst, J. K. In *Molecular Electronics—Science and Technology*: *Aviram*, A., Ed.; Engineering Foundation Press: New York, 1989; pp 385–392.
(48) Hammarström, L.; Almgren, M.; Norrby, T. *J. Phys. Chem.* **1992**, *96*, 5017–5024.